

Analysis of Typhoon Wind-Resistant Tapered Low-Rise Structure Using Computational Fluid Dynamics Simulation

Icon S. Quiambao^{1,*}, Alyssa Gail F. Alzaga¹, Alexander B. De Lara¹, Gilford B. Estores¹,
Ria Liza C. Canlas²

¹School of Civil, Environmental & Geological Engineering, Mapúa University, Philippines

²Po Lite Technology Inc., National University, Manila, Philippines

Received December 6, 2022; Revised March 6, 2023; Accepted April 7, 2023

Cite This Paper in the Following Citation Styles

(a): [1] Icon S. Quiambao, Alyssa Gail F. Alzaga, Alexander B. De Lara, Gilford B. Estores, Ria Liza C. Canlas, "Analysis of Typhoon Wind-Resistant Tapered Low-Rise Structure Using Computational Fluid Dynamics Simulation," *Civil Engineering and Architecture*, Vol. 11, No. 4, pp. 2100 - 2109, 2023. DOI: 10.13189/cea.2023.110430.

(b): Icon S. Quiambao, Alyssa Gail F. Alzaga, Alexander B. De Lara, Gilford B. Estores, Ria Liza C. Canlas (2023). *Analysis of Typhoon Wind-Resistant Tapered Low-Rise Structure Using Computational Fluid Dynamics Simulation*. *Civil Engineering and Architecture*, 11(4), 2100 - 2109. DOI: 10.13189/cea.2023.110430.

Copyright©2023 by authors, all rights reserved. Authors agree that this article remains permanently open access under the terms of the Creative Commons Attribution License 4.0 International License

Abstract Evolving climate conditions continue to intensify typhoon winds, whose threats and damage to civil structures usually result in heavy economic losses and casualties. Despite this, most low-rise structures continue to receive less inadequate considerations on lateral forces; hence, failure still occurs on these buildings during typhoons, and most of the damages are attributed to the phenomenon named vortex shedding. As low-rise buildings comprise the largest class of vulnerable structures, they likewise need to be adequately designed to resist wind forces as induced by vortex shedding. Hence, this study aims to analyze and develop a typhoon-resistant low-rise structural model, which will be tapered to reduce across-wind responses, through Computational Fluid Dynamics (CFD) Simulation. Po-Lite panels were considered in creating initial low-rise models, whose vortex shedding, and natural frequencies have then been identified through CFD using SimScale software and Finite Element Analysis (FEA) using MSC Patran and Nastran, respectively. The CFD simulation results indicate that the Circular Tapered Model showed the lowest mean lift and drag coefficients and lowest vortex shedding frequencies for each meter height interval as compared with other models. Similarly, Modal Analysis in FEA yielded values on the models' natural frequencies and modal shapes, and only the Circular Tapered Model showed no coinciding

vortex shedding and natural frequencies, indicating that no structural collapse occurs during the simulated typhoon winds. As a result, the study considers this geometry to be the governing low-rise Po-Lite model that can resist and adapt to the increasing intensities of typhoon wind loads. To better address other limitations, the study recommends that future studies employ wind tunnel tests, investigate medium- and high-rise structures, and apply different wind loading conditions, and consider the surrounding buildings in the analysis.

Keywords Typhoon Wind, Tapering, Computational Fluid Dynamics, Vortex Shedding Frequency, Finite Element Analysis, Natural Frequency

1. Introduction

Evolving climate conditions are continually exacerbating the intensity and severity of extreme wind events [1, 2], particularly typhoons, whose threats and damage to civil structures usually result in substantial economic losses and heavy casualties [3]. Low-rise non-engineered buildings comprise the largest class of vulnerable civil structures [4], but despite multiple findings

indicating the considerable damage of typhoon winds on these establishments [5], most wind studies focus more on high-rise structures [6], while low-rise buildings receive relatively less rigorous engineering design, accompanied by inadequate considerations on lateral force effects – in particular, they have only been generally employed with traditional practices that carry gravity loads but still lack in design against non-gravity loadings [7]. Recent studies describing the basic wind flow around a low-rise building [8] show that structural damage initiated in the roof regions is often attributed to the rows of wind vortices that are alternatively shed and periodically generated at the wake regions of buildings – a wind phenomenon called “vortex shedding” [9]. Building failure due to vortex shedding occurs when the vibrations of wind vortices coincide with the natural frequency of a building. In this regard, tapering structures, where the building sectional area is progressively decreased from the bottom to the top, can essentially optimize the structure’s aerodynamic behavior in controlling wind-induced vibrations. Wind forces and coefficients are usually measured through simulation tools such as Computational Fluid Dynamics (CFD) [10], and they constitute a useful basis for structural wind analysis for Finite Element Analysis (FEA) [11].

As typhoon winds continue to intensify due to climate changes, there remains an increasing need indicating the urgency for developing alternative structural solutions for low-rise structures in resisting extreme wind forces. In response to this problem, this study aimed to analyze and develop a low-rise structural model tapered to an optimal geometry for resisting extreme typhoon winds through CFD Simulation with the help of FEA. Specifically, this study sought to answer the following: (1) What are the significant force coefficients of wind flow that subject low-rise structures during typhoons? (2) What is the vortex shedding frequency of the typhoon wind vortices around traditional and tapered low-rise structures? (3) What is the fundamental frequency of vibration of traditional and tapered structural systems? (4) How does tapering the geometry of the structure affect the incidence of vortex shedding? And (5) What is the most optimum tapered geometry for a low-rise structure in resisting typhoon wind speeds?

2. Materials and Methods

Experimental simulations assisted the researchers in investigating the behavior of the models when subjected to wind loading conditions, as well as how the wind behaves when it contacts the face of the structure. In this study, the SimScale software was utilized to carry out the CFD simulation of wind flow while the MSC Patran and Nastran software was used to employ FEA on the structural models. The use of CFD simulation enabled the researchers to predict and identify the wind flow patterns around a building and identify the wind vortices’

frequency without the need to conduct expensive wind tests using limited facilities and instruments in the country. Meanwhile, the use of MSC Patran and Nastran for FEA allowed the researchers to obtain results that specified the fundamental frequencies of vibration, or natural frequencies, of certain models through modal analysis. Figure 1 shows the overall phase-by-phase flow of how the methodology of the study is conducted.

2.1. Phase 1: Creation of Structural Models

The architectural layout of tapered structures and their baselines were first imported to SimScale and MSC Patran. The AutoCAD software was used in preparing the models for the four types of low-rise structures utilized in the study, namely Rectangular, Pyramidal Hipped Roof, 4-Tapered, and Circular Tapered Structures, all having equivalent dimensions, floor areas, height, and number of stories.

2.2. Phase 2: Setting of Parameters

This phase includes specifying the parameters involved in the loadings of the structure – specifically, typhoon wind load coefficients and characteristics. Adopting the maximum wind speed of Super Typhoon Odette (Rai) of 260 kph, the parameters considered for CFD wind simulation were as follows: (1) Gust Effect Factor; (2) Velocity Pressure Coefficients; and (3) Velocity Pressure. Meanwhile, the mechanical properties of Po-Lite panel used in FEA were indicated to be 620.87 MPa for Elastic Modulus, 0.25 for Poisson Ratio, and 1527.27 kg/m³ for Density.

2.3. Phase 3: Analysis and Investigation through CFD and FEA

Extreme wind flow was modelled in SimScale using the set parameters, and this predicted the frequency of the generated vortices by the simulated wind flow through Incompressible LBM Solver. Upon obtaining the results, the natural frequency of the models was acquired through modal analysis in MSC Patran and Nastran. For CFD simulation, the pre-processing phase involved (1) importing the structural models or geometry developed from AutoCAD into the SimScale platform and (2) setting up the solution domain, meshing, material properties, and boundary conditions for the wind simulation. In preparing the computational domain, the present study followed the recommendations from [12], indicating that the inlet and top boundary was located 5H away from the structure while the outlet was positioned at 15H, where H is the building height. The boundary conditions which comprise the inflow, outflow, and wall boundaries were set based on a similar study by [9], taking note of the new set parameters for this study. Meanwhile, the pre-processing

phase for Modal Analysis in FEA also included the considerations for meshing, material properties, and boundary conditions, wherein the models were constrained at the bottom, signifying a fixed support. No loads were included in determining the natural frequencies of the models.

2.4. Phase 4: Optimization and Development of the Selected Model

The natural frequencies of the structure obtained using MSC Patran and Nastran were compared to the frequency of vortex shedding as determined by the CFD wind simulation. The model with the least coinciding frequencies between the two was selected. Optimizing the selected model was also an option to achieve the desired model of the study.

2.5. Phase 5: Evaluation Procedure

The CFD results of the frequency of vortex shedding were compared with the approximated fundamental frequency of the structure. Section 207.9 of the NSCP 2015 presents the equations needed in the estimation of the dynamic response of the structures.

3. Results and Discussion

3.1. CFD Simulation of the Models

3.1.1. Velocity Profiles

The velocity profile of the structural models in the simulation provides information about the flow of fluid – in this case, air – within a structure. This information can be used to determine if there are areas of high velocity, low velocity, or no flow at all. To visualize the turbulence of the air flowing through the wind tunnel, a cutting plane along the Y-axis was taken exactly at the center of each structural model. Observing the flow patterns on the figures presented below, the Rectangular-Shaped, Pyramidal, and 4-Tapered models (Figures 2-4) exhibited recirculation of air on the leeward side of the structure. High turbulence is also depicted in each velocity profile of the mentioned models as there are fluctuations in their velocity contours as represented by the abrupt shift in gradient – from yellow to blue. On the other hand, the Circular Tapered Model (Figure 5) exhibited the least turbulent flow as the contours of its velocity profile remain consistent throughout the simulation.

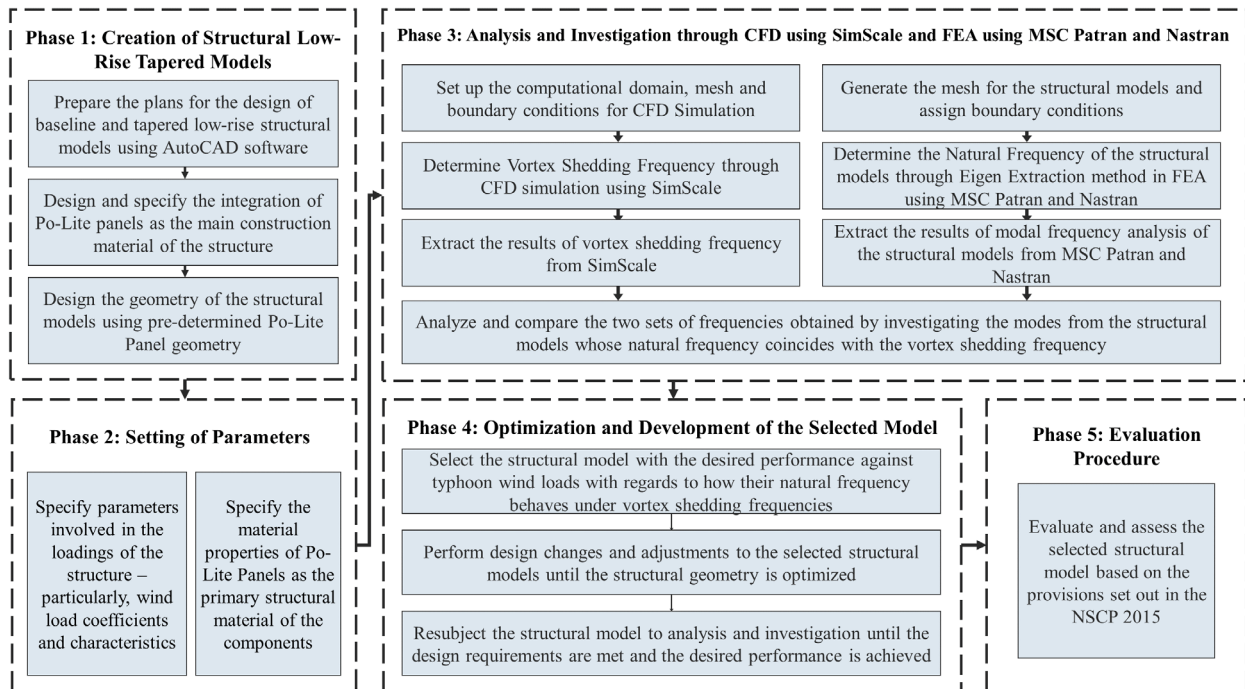


Figure 1. Methodology of the study

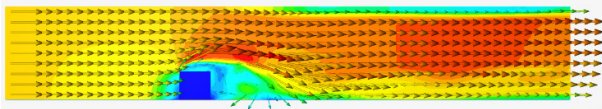


Figure 2. Velocity profile of Rectangular-shaped model

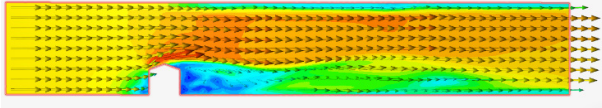


Figure 3. Velocity profile of Pyramidal hipped roof model

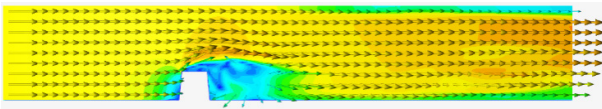


Figure 4. Velocity profile of 4-tapered model

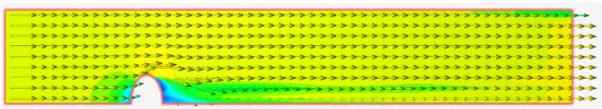


Figure 5. Velocity profile of Circular-tapered model

Comparing the contours of Rectangular, Pyramidal Hipped Roof and 4-Tapered models (Figures 2-4), it can be observed that the Rectangular and 4-Tapered models experienced an observable uplift on the top surface. The contours of the Pyramidal Hipped Roof Model (Figure 3) conform with the findings of [12] in which the said model exhibits a low uplift as compared to rectangular-shaped structures. However, considering the velocity profile of the Circular Tapered Model (Figure 5), the velocity contours on its profile exhibited minimal fluctuations and its speed stayed consistent in range. Thus, it is indicative that it yielded a minimal to no recirculation of air as well as any uplift.

3.1.2. Turbulent Kinetic Energy

A cutting plane along the Y-Axis was positioned along the center of the structure to monitor the behavior of the turbulent flow along the structure. The profile was taken at $t = 240$ seconds to show the distinct turbulent flow occurring on each model. Consequently, the scales were calibrated such that all contours have distinct values for each time iteration. A red contour on the profile signifies maximum turbulent kinetic energy while solid blue contours denote minimal to zero kinetic energy. The values for the turbulent kinetic energy of the models along the cutting plane were recorded. As shown in Table 1, the Rectangular-Shaped model (Figure 6a) yielded a maximum value of $251.7 \text{ m}^2/\text{s}^2$. For the Pyramidal Hipped Roof model (Figure 6b), the turbulent kinetic energy profile recorded a maximum of $142.1 \text{ m}^2/\text{s}^2$. The 4-Tapered model (Figure 6c), on the other hand, had the greatest turbulent kinetic energy value among all models, having

$385.3 \text{ m}^2/\text{s}^2$. Lastly, the Circular Tapered model (Figure 6d) had the best response to turbulent flow as it yielded the least value for the turbulent kinetic energy of $54.88 \text{ m}^2/\text{s}^2$.

Table 1. Turbulent Kinetic Energy Values

Model	Turbulent Kinetic Energy (m^2/s^2)
01 Rectangular	251.70
02 Pyramidal	142.10
03 4-Tapered	385.30
04 Circular Tapered	54.88

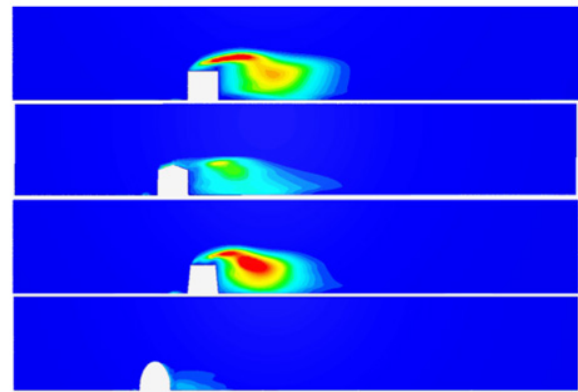


Figure 6. Turbulent Kinetic Energy Profiles of (a) Rectangular-shaped, (b) Pyramidal, (c) 4-tapered, and (d) Circular tapered models

3.1.3. Lift Coefficients

Presented in Fig. 7 is the time series plot for the models during the time interval of 30 seconds to 300 seconds. It is noticeable that the Pyramidal Hipped Roof model sustained the highest values for the lift coefficient while the Circular Tapered model had the lowest values for the lift coefficient. The Pyramidal Hipped Roof model exhibited the highest mean lift coefficient among the four models with a value of $C_L = 0.7856766$, while the Circular-Tapered model had the lowest mean lift coefficient of $C_L = 0.0514535$. The values of the mean lift coefficient for the first three models are relatively close to one another while that of the Circular Tapered model is substantially farther apart.

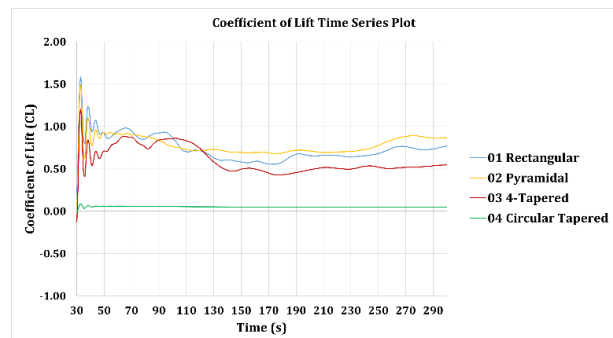


Figure 7. Coefficient of Lift Time Series Plot

3.1.4. Drag Coefficients

In this parameter, the Rectangular-Shaped model exhibited the highest mean drag coefficient of $C_D = 1.4327467$, whereas the Circular Tapered model had the least value for the mean drag coefficient with value averaging at $C_D = 0.0240405$. Both 4-Tapered and Circular Tapered models exhibited lower drag coefficients compared to the traditional geometries of Rectangular and Pyramidal Hipped Roof wherein the coefficient of drag for the 4-Tapered structure is 1.0532729 and 0.0240405 for the Circular Tapered model. The rectangular model yielded a drag coefficient of 1.4327467 while the pyramidal model had a drag coefficient of 1.1968505. The result in this study conforms to previous findings which suggested that tapering the profile of the structure plays a significant role in the reduction of the drag coefficient on the structure – thus, improving the aerodynamic behavior of the structure.

3.1.5. Mean Force Coefficients

Assessing both mean coefficients of lift and drag as presented in Table 2, it is indicative that the Circular Tapered model had the best aerodynamic response on the wind speed as it yielded the lowest values for both lift and drag coefficients.

Table 2. Mean Force Coefficients

Model	Mean Lift Coefficient (C_L)	Mean Drag Coefficient (C_D)
01 Rectangular	0.7432263	1.4327467
02 Pyramidal	0.7856766	1.1968505
03 4-Tapered	0.6021097	1.0532729
04 Circular Tapered	0.0514535	0.0240405

Table 3. Vortex Shedding Frequencies of the models

Height (m)	Rectangular	Pyramidal	4-Tapered	Circular Tapered
1	0.244	0.3204	0.4028	0.0057
2	0.5255	0.0984	0.3319	0.002756
3	0.077	0.0521	0.1536	0.000677
4	0.2322	0.04122	0.1242	0.01657
5	0.2915	0.05002	0.04821	0.01914
6	0.4647	0.0223	0.07727	0.01713

3.1.6. Vortex Shedding Frequency

The vortex shedding frequency of a structure can be obtained by acquiring the vorticity contours of the models during the simulation [13]. A cutting plane along the Z-axis

of the models was taken at every 1-meter interval from the base of the models. The average vorticities (measured in Hz) of the models were taken for each cutting plane generated along the models. Summarized in Table 3 are the frequencies of vortex shedding at a given height for the four models in the study.

The frequencies of vortex shedding were lowest for the Circular Tapered model in comparison to the other three models. On the other hand, the Rectangular and 4-Tapered models had the highest shed vorticities among the four models. It is worth noting that the 4-Tapered model also yielded high frequencies of vortex shedding as compared with the Circular Tapered and Pyramidal models. It is also important to consider that both Rectangular and 4-Tapered models exhibited the greatest turbulence among the four models. The results of this investigation are consistent with the findings of previous studies, which suggest that reducing turbulent kinetic energy leads to considerable suppression of vortex shedding on the structure.

3.2. Modal Analysis

The structural solid models, subject to FEA, were imported to MSC Patran and Nastran. The meshing of the models was done prior to assigning the boundary conditions. The rectangular-shaped model was meshed with Hex elements (IsoMesh type), while the pyramidal, 4-Tapered, and circular tapered were meshed with Tet elements (TetMesh type) due to the complexity of the structures. Figures 8-11 show the meshing of the structural models as performed in MSC Patran:

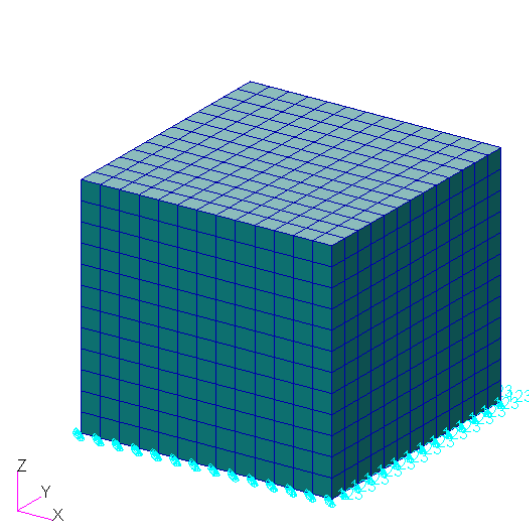


Figure 8. Meshing of Rectangular-shaped model

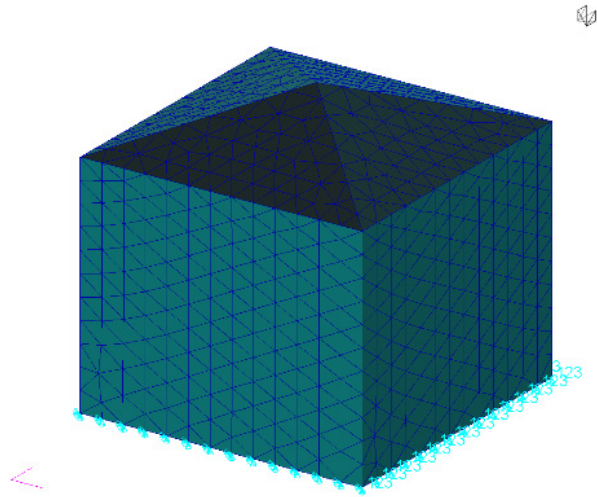


Figure 9. Meshing of Pyramidal hipped roof model

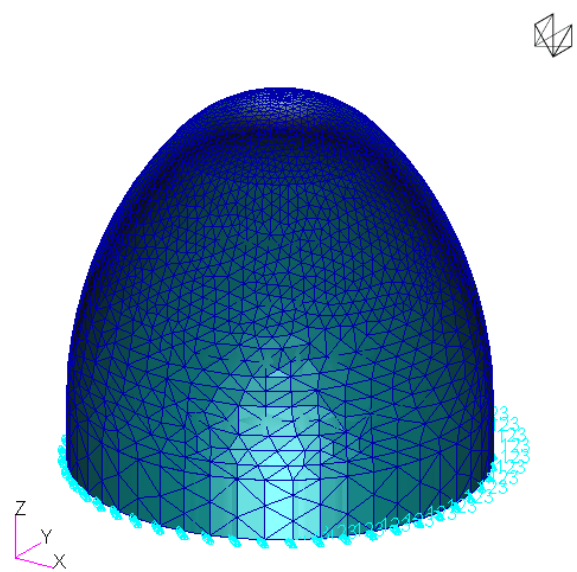


Figure 11. Meshing of Circular tapered model

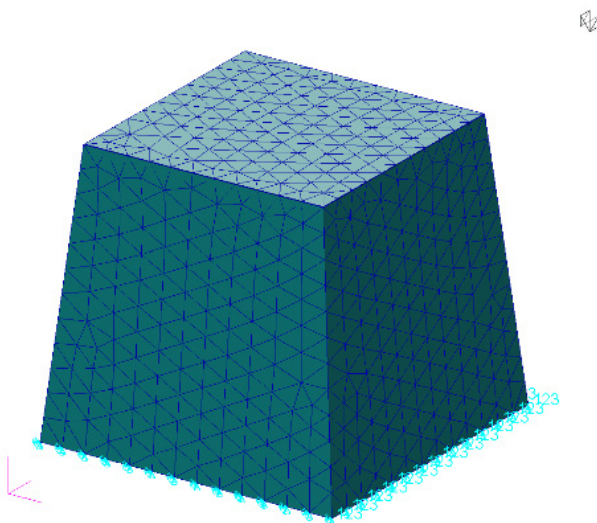


Figure 10. Meshing of 4-tapered model

The natural frequency (in Hz) is obtained from the modal analysis, along with the mode shape and mode number of the structure. A total of 10 mode shapes per model was investigated, and the results are presented herein (Figure 12). The modal shapes indicate how the structure will tend to deform at specific natural frequencies as well as the regions where the greatest stresses will be experienced once the structure deformed similarly with the specified modal shape.

Through modal analysis, the natural frequencies of the structural models are obtained, which are subject to comparison with the vortex shedding frequencies from CFD wind simulation to check the regions with coinciding frequencies that will indicate failure or collapse. Tables 4-7 show the corresponding natural frequencies and eigenvalues for each structural model of the study.

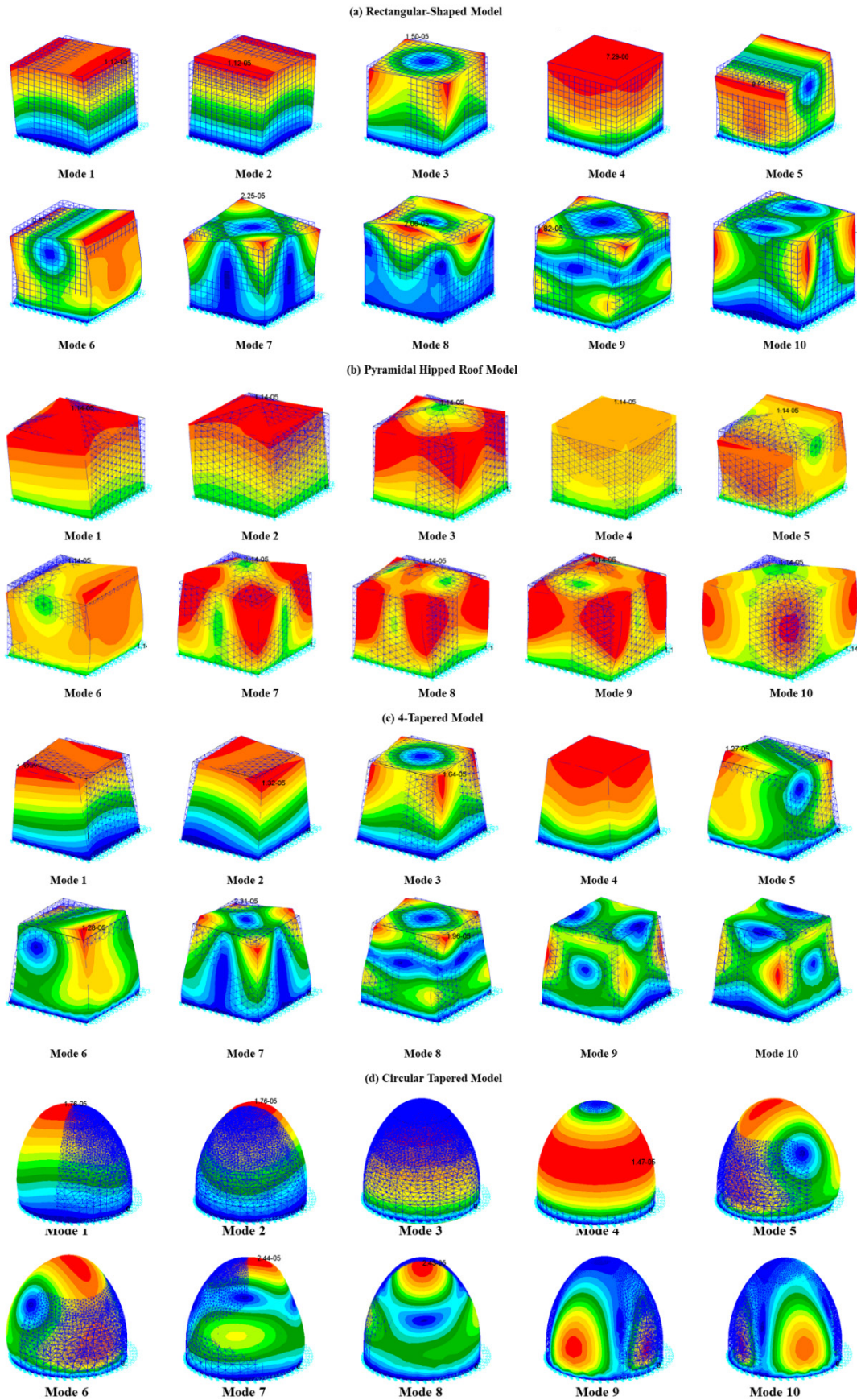


Figure 12. Modal shapes after performing Modal Analysis of (a) rectangular-shaped, (b) pyramidal hipped roof, (c) 4-tapered, and (d) circular tapered models

Table 4. Natural Frequencies of Rectangular-shaped model

Mode	Natural Frequency	Eigenvalue
1	0.2356	2.1913
2	0.2356	2.1913
3	0.33948	4.5497
4	0.38661	5.9008
5	0.48648	9.3432
6	0.48648	9.3432
7	0.81477	26.208
8	0.99386	38.995
9	1.0141	40.601
10	1.0194	41.027

Table 5. Natural Frequencies of Pyramidal hipped roof model

Mode	Natural Frequency	Eigenvalue
1	0.2575	2.6172
2	0.2607	2.6828
3	0.3738	5.5175
4	0.4196	6.9516
5	0.5267	10.9534
6	0.5296	11.0723
7	0.9227	33.6136
8	1.0453	43.1324
9	1.0481	43.3656
10	1.0698	45.1810

Table 6. Natural Frequencies of 4-tapered model

Mode	Natural Frequency	Eigenvalue
1	0.2693	2.8621
2	0.2728	2.9379
3	0.4095	6.6199
4	0.4231	7.0671
5	0.5394	11.4862
6	0.5409	11.5511
7	0.9863	38.4051
8	1.0675	44.9913
9	1.1395	51.2586
10	1.1433	51.6063

Table 7. Natural Frequencies of Circular-tapered model

Mode	Natural Frequency	Eigenvalue
1	0.34314	4.6483
2	0.34492	4.6967
3	0.50419	10.036
4	0.56109	12.429
5	0.63224	15.78
6	0.63422	15.88
7	1.3221	69.004
8	1.3239	69.197
9	1.3278	69.605
10	1.3293	69.762

The modal participation factors for each model are determined. The results for each translational degrees of freedom (Table 8) in the x-, y-, and z-directions (T1, T2, T3), as well as rotational degrees of freedom (Table 9) in the x-, y-, and z-directions (R1, R2, R3), of each model, with a reference point at the origin of basic coordinate system, are outlined as follows. Since the total effective mass of all models in each direction exceeds the desired threshold of 90% modal effective mass, the number of modes extracted in the normal modes analysis can be deemed significant.

Table 8. Modal participation factors of models (Translational)

Model	T1	T2	T3
Rectangular	96.93%	96.89%	97.90%
Pyramidal	96.13%	96.18%	97.17%
4-Tapered	95.71%	95.76%	96.88%
Circular Tapered	96.53%	96.53%	96.82%

Table 9. Modal participation factors of models (Rotational)

Model	R1	R2	R3
Rectangular	97.91%	97.95%	96.93%
Pyramidal	97.50%	97.50%	94.83%
4-Tapered	96.87%	96.95%	95.69%
Circular Tapered	98.44%	98.47%	90.05%

It was found out that the rectangular-shaped, pyramidal hipped roof, and 4-tapered structures have coinciding frequencies from heights ranging from 1 to 6 meters. Moreover, the rectangular and 4-tapered models obtained the highest vortex shedding frequencies, while the circular tapered model obtained the lowest values. This means that the vortex shedding observed in the circular tapered model has the lowest chance of causing failure to structure, as the structure also showed no coinciding natural frequencies of vibration with the vortex shedding frequencies.

As the natural frequencies obtained in MSC Patran and Nastran from the circular tapered structure did not coincide with the values in the frequencies from vortex shedding in CFD analysis, as well as the approximated fundamental frequency in the NSCP 2015, the study can identify the circular tapered structure as the most optimum tapered geometry among the established low-rise structural models.

4. Conclusions

In analyzing the low-rise structural models' response to typhoons, the study first identified the significant wind force coefficients that subject these structures during strong winds. Among the models, the pyramidal hipped roof model exhibited the largest mean lift coefficient of $C_L = 0.7857$, while the rectangular-shaped structure showed the highest mean drag coefficient of $C_D = 1.43277$. For both parameters, the Circular-Tapered model exhibited the lowest mean lift and mean drag coefficients of $C_L = 0.0515$ and $C_D = 0.0240$, respectively. These results agree with the recent studies that tapering the geometry can reduce drag coefficients.

By cutting a plane at the Z-axis of the models during the simulation, their vortex shedding frequencies were obtained through their vorticity contours. The Circular Tapered model showed the lowest vortex shedding frequencies compared to the other models. These frequencies are attributed to the amount of vortex shedding induced upon the subsection of the structures to wind loads – the greater the vortex shedding, the higher the frequency.

Upon determining the vortex shedding frequencies, the extracted modal shapes which indicate the structure's potential deformation at specific natural frequencies are then investigated; wherein, natural frequencies which coincide with the vortex shedding frequency indicate a possible collapse or failure. Through modal analysis, the natural frequencies of the models have been obtained in 10 modal shapes. The total effective mass of all structural models in each direction have exhibited modal participation values greater than the desired threshold of 90%; hence, this indicates that the number of modal shapes in the analysis, initially identified to be ten (10), is significant in all models.

Among the four structures, only the natural frequencies of the Circular Tapered structure did not coincide with the vortex shedding frequencies, while the remaining models indicated otherwise that failure and collapse can potentially occur in certain regions of these structures.

Given that the Circular Tapered model showed the most desirable response among the four models and exhibited no coinciding frequencies, it was selected as the final tapered structural model, which the study identifies to have the most optimum geometry for resisting typhoon wind loads. Furthermore, the following recommendations are hereby

made: (1) use the Circular-Tapered Model as a structural geometry to withstand high wind speeds to better dissipate the wind caused by typhoons; (2) employ wind tunnel analysis to overcome the constraints of the study on wind tunnel testing; (3) the researchers further recommend opting for a transient solution to the simulation to account for the time-dependent effects that may vary with respect to time; (4) vary the meshing parameters of the conducted FEA to better illustrate the behavior of each element in the mesh; (5) consider conducting the study on medium-rise structures as well as high-rise structures; and (6) consider the physical and environmental urban contexts of the building, including the surrounding buildings' heights, sizes, topography and land cover, in the typhoon wind analysis.

Acknowledgements

The study would not have been completed without the guidance and expertise of the following: Engr. Edgardo S. Cruz and Engr. Yoshiaki C. Mikami for providing insightful recommendations about the study; Dr. Ria Liza C. Canlas of Po-Lite Technology Inc., for giving the opportunity and providing information resources to this paper; and Engr. Vicente S. Dy Reyes and Dr. Andre S. Publico for providing training on how the researchers can utilize the Finite Element Analysis (FEA) using MSC software. The researchers also gratefully acknowledge the Department of Science and Technology (DOST) for aiding in the research expenses.

REFERENCES

- [1] G. Y. Kim, S. Lee. Prediction of extreme wind by stochastic typhoon model considering climate change, *Journal of Wind Engineering & Industrial Aerodynamics*, Vol.192, 2019.
- [2] T. Dinan. Projected increases in hurricane damage in the United States: The role of climate change and coastal development, *Ecological Economics*, Vol.138, 186-198, 2017.
- [3] Q.S. Li, J. C. Li, S.Y. Hu. Monitoring of near-surface winds and wind pressures on an instrumented low-rise building during Super Typhoon Rammasun, *Journal of Structural Engineering*, Vol.145, 2019.
- [4] W. Zhang, P. Gruber. Wind-resilient civil structures: What can we learn from nature, *Botany*, Vol.98, 37-48, 2019.
- [5] Y. C. He et al. Insights from Super Typhoon Mangkhut (2013) for wind engineering practices, *Journal of Wind Engineering & Industrial Aerodynamics*, Vol.203, 2020.
- [6] Q. S. Li, X. Li, Y. He, J. Yi. Observation of wind fields over different terrains and wind effects on a super-tall building during a severe typhoon and verification of wind tunnel predictions, *Journal of Wind Engineering and Industrial*

Aerodynamics, Vol.162, 73-84, 2017.

- [7] J. He, F. Pan, C.S. Cai. A review of wood-frame low-rise building performance study under hurricane winds, *Engineering Structures*, Vol.141, 512-529, 2017.
- [8] A. M. Aly, F. Khaled, H. Gol-Zaroudi. Aerodynamics of low-rise buildings: Challenges and recent advances in experimental and computational methods, in *Aerodynamics*, M. Gorji-Bandpy and A. Aly, Eds., 2020.
- [9] C. V. Okafor. Finite element analysis of vortex induced responses of multistory rectangular building, *European Journal of Engineering Research and Science*, Vol.3, 2018.
- [10] J. He, F. Pan, C. S. Cai, F. Habte, A. Chowdhury. Finite-element modeling framework for predicting realistic responses of light-frame low-rise buildings under wind loads, *Engineering Structures*, Vol.164, 53-69, 2018.
- [11] C. V. Okafor. Application of computational fluid dynamics model in high-rise building wind analysis: A case study, *Advances in Science, Technology and Engineering Systems*, Vol.2, 197-203, 2017.
- [12] J. Singh, A. K. Roy. Effects of roof slope and wind direction on wind pressure distribution on the roof of a square plan pyramidal low-rise building using CFD simulation, *International Journal of Advanced Structural Engineering*, Vol.11, 231–254, 2019.
- [13] X. J. Wang, Q. S. Li, B. W. Yan, J. C. Li. Field measurements of wind effects on a low-rise building with roof overhang during typhoons, *Journal of Wind Engineering & Industrial Aerodynamics*, Vol.176, 143–157, 2018.